

# Cross-Sectional and Longitudinal Assessment of Retinal Sensitivity in Patients With Childhood-Onset Stargardt Disease

Preena Tanna<sup>1,2,\*</sup>, Michalis Georgiou<sup>1,2,\*</sup>, Jonathan Aboshiha<sup>1,2</sup>, Rupert W. Strauss<sup>1-3</sup>, Neruban Kumaran<sup>1,2</sup>, Angelos Kalitzeos<sup>1,2</sup>, Richard G. Weleber<sup>4</sup>, and Michel Michaelides<sup>1,2</sup>

<sup>1</sup> UCL Institute of Ophthalmology, University College London, London, UK

<sup>2</sup> Moorfields Eye Hospital, London, UK

<sup>3</sup> Departments of Ophthalmology, Kepler University clinic Linz and Medical University Graz, Graz, Austria

<sup>4</sup> Casey Eye Institute, Oregon Health & Science University, Portland, OR, USA

**Correspondence:** Michel Michaelides, UCL Institute of Ophthalmology, 11-43 Bath St, London, EC1V 9EL, UK. e-mail: michel.michaelides@ucl.ac.uk  
Richard Weleber, Casey Eye Institute, Oregon Health & Science University, Portland, OR, USA. e-mail: weleberr@ohsu.edu

**Received:** 9 January 2018

**Accepted:** 26 September 2018

**Published:** 27 November 2018

**Keywords:** Retinal sensitivity; perimetry; visual field; retina; Stargardt disease; *ABCA4*; STGD1; clinical trials; endpoints

**Citation:** Tanna P, Georgiou M, Aboshiha J, Strauss RW, Kumaran N, Kalitzeos A, Weleber RG, Michaelides M. Cross-sectional and longitudinal assessment of retinal sensitivity in patients with childhood-onset Stargardt disease. *Trans Vis Sci Tech.* 2018;7(6):10, <https://doi.org/10.1167/tvst.7.6.10>  
Copyright 2018 The Authors

**Purpose:** We assess cross-sectional and longitudinal microperimetry and full-field static perimetry-derived retinal sensitivity with conventional and volumetric indices of retinal function in childhood-onset Stargardt disease (STGD1).

**Methods:** Subjects with molecularly confirmed childhood-onset STGD1 underwent full-field static perimetry and/or microperimetry using custom designed grids. Mean sensitivity (MS) and total volume ( $V_{TOT}$ ) were computed for each microperimetry test. MS,  $V_{TOT}$ , and central field volume ( $V_{30}$ ) were computed for each full-field static perimetry test. Subjects under 18 years old at baseline were classified as children and subjects 18 years or older as adults.

**Results:** A total of 43 children (mean age at baseline, 13.0 years; range, 8–17) and 13 adults (mean age at baseline, 23.1 years; range, 18–32) were included in the analysis. For full-field static perimetry and microperimetry for both subgroups, intraclass correlation coefficient results for MS and volumetric indices were good to excellent, indicating strong test–retest reliability. Interocular symmetry in terms of baseline measurements and the annual rate of progression was observed. A greater rate of progression was observed in childhood.

**Conclusions:** To our knowledge, this is the first prospective study of retinal sensitivity in a large cohort of molecularly confirmed subjects with childhood-onset STGD1 demonstrating that children with STGD1 can reliably undertake detailed functional testing. Moreover, using custom designed grids and subsequent topographic analysis, volumetric indices of retinal function provide a reliable measure of retinal sensitivity.

**Translational Relevance:** This study highlights the use of microperimetry and full-field static perimetry, as well as volumetric indices of retinal function, in monitoring disease progression.

## Introduction

Stargardt disease (STGD1; MIM 248200) is the most common inherited macular dystrophy in adults and children, with a prevalence of 1 in 8000–10,000.<sup>1–7</sup> STGD1 has an autosomal recessive mode of inheritance associated with disease-causing mutations in the *ABCA4* gene.<sup>1,8–11</sup> Onset is most commonly in child-

hood, with subjects presenting with bilateral central visual loss and characteristic macular atrophy with yellow–white flecks at the level of the retinal pigment epithelium (RPE) at the posterior pole.<sup>1–3,5,12,13</sup> There is progressive loss of retinal function and structure over time, which varies significantly within and between the three principal groups of STGD1: namely childhood-onset, adult-onset, and late-onset/foveal sparing

STGD1.<sup>1,14–19</sup> There are no proven treatments, yet STGD1 is subject to more clinical trials than any other inherited retinal disease; gene replacement, stem cell therapy, and pharmacologic approaches currently are being investigated.<sup>1,5,20–23</sup>

Identifying the most suitable method of assessing retinal function, in particular retinal sensitivity, is crucial for the design of any treatment strategy. Clinical studies with a cross-sectional design have shown that microperimetry is a reliable measure of macular sensitivity in subjects affected by macular diseases, including *ABCA4*-retinopathy.<sup>24–26</sup> Full-field static perimetry provides an assessment of retinal sensitivity including and beyond the central retina. Although the current understanding of full-field static perimetry testing in subjects with STGD1 is limited, it would be valuable to assess retinal sensitivity in regions of interest outside the limits of microperimetry. For instance, it has been suggested that the peripapillary area is a retinal region of interest for monitoring the efficacy of treatments in *ABCA4*-associated retinal degenerations.<sup>27</sup> Moreover, a significant proportion of subjects with STGD1 have involvement beyond the central retina, including the majority of childhood-onset STGD1 subjects who have additional generalized retinal involvement.<sup>1,4</sup>

Reliable outcome measures also are crucial for an accurate representation of retinal function. Microperimetry and full-field static perimetry data are summarized conventionally by a single global index, such as mean sensitivity (MS), which simply is the average sensitivity value of all retinal locations tested. However, static perimetry data also can be summarized using topographic models and volumetric indices of function to quantify the magnitude and extent of the visual field sensitivity.<sup>28</sup> Topographically-derived indices represent the volume of sensitivity that is useful when describing retinal functional progression over time<sup>28</sup> and, therefore, valuable for clinical management and the design of treatment trials.

We assessed cross-sectional and longitudinal microperimetry and full-field static perimetry-derived retinal sensitivity with conventional and volumetric indices of retinal function in childhood-onset STGD1. We explored test–retest reliability, interocular symmetry, and rate of progression over time.

## Methods

This ethically approved study was undertaken at the Clinical Research Facility at Moorfields Eye Hospital and at the UCL Institute of Ophthalmology.

The Declaration of Helsinki was adhered to throughout the study.

## Subjects

Molecularly confirmed STGD1 subjects were tested as part of an ongoing natural history study whereby the study was explained and consent was obtained. Subjects younger than 18 years at baseline were classified as children and subjects 18 years or older as adults. All adults had documented evidence of childhood-onset STGD1.

## Full-Field Static Perimetry

Full-field static perimetry was performed monocularly using the Octopus900 (Haag-Streit AG, Köniz, Switzerland). Fixation was monitored by a dedicated ophthalmic technician throughout each assessment. Testing consisted of a 31.4 apostilbs (10 cd/m<sup>2</sup>) background, Goldmann size V stimulus presented for a duration of 200 ms, and the German Adaptive Thresholding Estimation (GATE) strategy, which has a shorter testing duration compared to conventional full-threshold strategies.<sup>29</sup> The customized testing grid consisted of 185 testing locations. The grid pattern was oriented radially, centrally condensed, and binocularly symmetric ([Supplementary Fig. S1](#)). An MS value was automatically computed for each test by the manufacturer's inbuilt software (EyeSuite). The quality of each test was evaluated based on the reliability factor (RF), the percentage of total catch trials resulting in either a false-positive or false-negative. Any test with an RF >30% was excluded.

## Microperimetry

Microperimetry was performed monocularly using the Nidek MP-1 (Nidek Technologies, Padova, Italy). Pupils were dilated and cyclopleged using 2.5% phenylephrine hydrochloride solution (Bausch & Lomb, Inc., Tampa, FL) and 1% tropicamide ophthalmic solution (Akorn, Inc., Lake Forest, IL). Fixation was monitored by a dedicated ophthalmic technician throughout each assessment. Before testing, the Spectralis OCT (Heidelberg Engineering, Heidelberg, Germany) was used to obtain a single transfoveal horizontal line scan. This was imported and used by the Nidek MP-1 manufacturer's software as an aid to automatically locate the anatomic fovea to facilitate accurate foveal placement of the testing grid. Testing consisted of a 4 apostilbs (1.27 cd/m<sup>2</sup>) background, Goldmann size III stimulus presented for a duration of 200 ms, and a 4 to 2 dB full-

threshold bracketing test strategy. The customized testing grid consisted of 44 testing locations. The grid pattern was of radial design with centrally-condensed spacing and covered the macular and paramacular regions (Supplementary Fig. S2). An MS value was computed automatically for each test by the manufacturer's software.

## Volumetric Indices of Retinal Function

Volumetric indices were derived from topographic analysis using Visual Field Modelling and Analysis (VFMA; Office of Technology Transfer & Business Development, Portland, OR), a custom software application.<sup>28</sup> The volumetric indices derived included the total volume ( $V_{TOT}$ ), which represented the entire tested field, and the central field volume ( $V_{30}$ ), defined by a central circle with a radius of 30°. The volume represents the total sensitivity across the solid angle of the base of the test grid for  $V_{TOT}$  and the solid angle of a 30° radius circle selection for  $V_{30}$ , and is reported in units of decibel-steradians (dB-sr).<sup>28</sup> Sensitivity data from all perimetry tests were extracted for subsequent topographic analysis.  $V_{TOT}$  and  $V_{30}$  were computed for each full-field static perimetry test.  $V_{TOT}$  was computed for each microperimetry test.

## Determination of Test–Retest Reliability, Interocular Symmetry, Rate of Progression, Perimetry Correlations, and Statistical Methods Used

For full-field static perimetry and microperimetry, the subgroup of childhood-onset STGD1 <18 years and the comparatively smaller childhood-onset STGD1 subgroup aged ≥18 years at baseline were analyzed separately. The statistical analysis was performed with MS,  $V_{TOT}$ , and  $V_{30}$  results for full-field static perimetry tests, and with MS and  $V_{TOT}$  results for microperimetry tests.

Statistical analysis was performed using SPSS Statistics (Chicago, IL). Significance for all statistical tests was set at  $P < 0.05$ . The Shapiro-Wilk test was used to test for normality for all variables. Test–retest reliability was investigated with the intraclass correlation coefficient (ICC) based on absolute agreement and a 2-way mixed-effects model using results from the left eye to minimize the clustering effect. The annual rate of progression in sensitivity was calculated for each subject based on the total change in sensitivity over the total follow-up. The difference between eyes in the baseline measurement and the annual rate of progression was assessed in subjects

with bilateral data using the paired *t*-test to evaluate functional symmetry and the correlation between eyes was assessed with the Pearson's correlation coefficient. The independent *t*-test was used to determine if there was a significant difference in the rate of progression between children and adults. The correlation between baseline MS and  $V_{TOT}$  from microperimetry and full-field static perimetry, for adults and children, was tested using the Pearson correlation coefficient.

## Results

A total of 43 children (mean age at baseline, 13.0 years; range, 8–17) and 13 adults (mean age at baseline, 23.1 years; range, 18–32) with molecularly confirmed childhood-onset STGD1 underwent full-field static perimetry and/or microperimetry testing. Figure 1 summarizes the subject data included in the study. All measured variables were normally distributed.

### Full-Field Static Perimetry

A total of 17 children and 10 adults with childhood-onset STGD1 underwent full-field static perimetry testing (Fig. 1). Two children with one baseline visit were unable to complete the full test on both eyes. Two children and 1 adult with one baseline visit had a RF of >30% for both eyes and, therefore, were excluded from the analysis.

### Test–Retest Reliability

Seven children (mean age at baseline, 15.3 years; range, 13–17) underwent full-field static perimetry testing twice at baseline. The ICC values in this subgroup for MS,  $V_{TOT}$ , and  $V_{30}$  were 0.86, 0.94, and 0.88, respectively.

Six adults with childhood-onset STGD1 (mean age at baseline, 26.3 years; range, 18–32) underwent full-field static perimetry testing twice at baseline. The ICC values in this subgroup for MS,  $V_{TOT}$ , and  $V_{30}$  were 0.89, 0.95, and 0.92, respectively.

### Interocular Symmetry

Data from nine children (mean age at baseline, 14.7 years; range, 13–16) and seven adults (mean age at baseline, 23.4 years; range, 18–32) with full-field static perimetry testing at least once on each eye and a minimum 12-month follow-up were analyzed to assess interocular symmetry.

The subgroup of children showed a strong correlation between eyes in the baseline measurements of MS ( $r = 0.98$ ),  $V_{TOT}$  ( $r = 0.98$ ), and  $V_{30}$  ( $r = 0.96$ ).

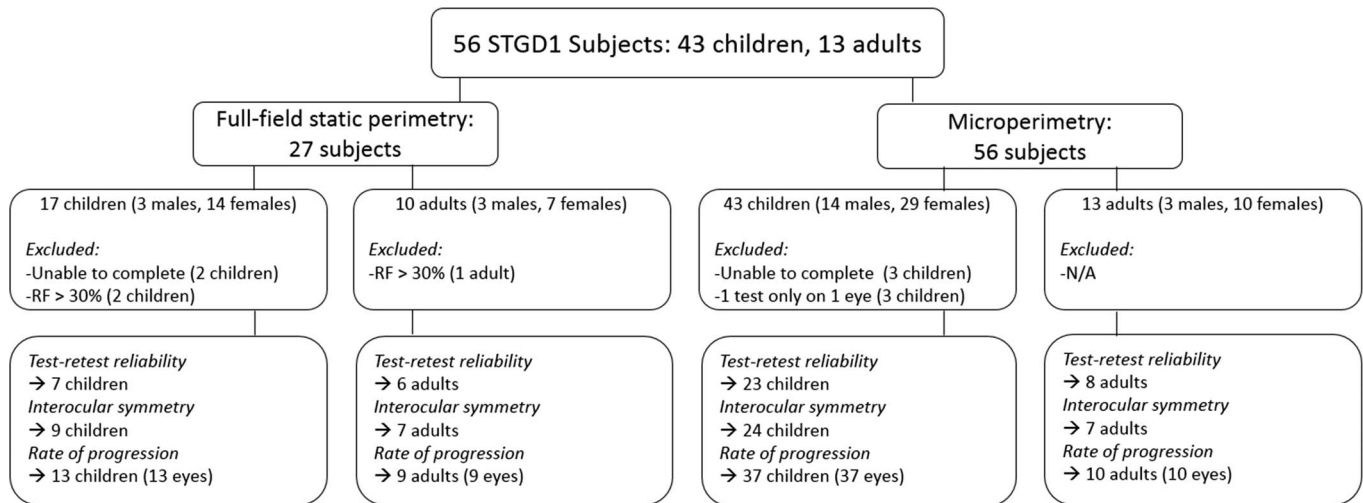


**Figure 1.** Flowchart summarizing assessments performed per patient subgroup. RF, reliability factor.

There also was a strong correlation between eyes in the annual rate of progression of MS ( $r = 0.87$ ),  $V_{TOT}$  ( $r = 0.85$ ), and  $V_{30}$  ( $r = 0.71$ ). There was no statistically significant difference between eyes in the baseline measurements of MS ( $P = 0.512$ , paired  $t$ -test) and annual rate of progression of MS ( $P = 0.099$ , paired  $t$ -test). **Figure 2A** shows a representative example of interocular symmetry.

The subgroup of adults showed a strong correlation between eyes in the baseline measurements of MS ( $r = 0.94$ ),  $V_{TOT}$  ( $r = 0.95$ ), and  $V_{30}$  ( $r = 0.93$ ). There also was a strong correlation between eyes in the annual rate of progression of MS ( $r = 0.88$ ),  $V_{TOT}$  ( $r = 0.89$ ), and  $V_{30}$  ( $r = 0.76$ ). There was no statistically significant difference between eyes in the baseline measurements of MS ( $P = 0.38$ , paired  $t$ -test) and annual rate of progression of MS ( $P = 0.853$ , paired  $t$ -test).

### Rate of Progression

Given the lack of statistically significant differences and strong correlations between eyes in the baseline measurements and annual rate of progression, subjects with baseline and follow-up full-field static perimetry testing on at least one eye were assessed subsequently to determine the annual rate of progression. For subjects with serial testing on both eyes, one eye was chosen at random. All subjects had a minimum follow-up of 12 months.

Thirteen eyes of 13 children (mean age at baseline, 15.4 years; range, 13–17) were included and had a mean follow-up of 27.1 months (range, 12–45 months). Mean baseline MS,  $V_{TOT}$ , and  $V_{30}$  were  $26.52 \pm 4.41$  dB,  $99.38 \pm 15.12$  dB-sr, and  $25.08 \pm 6.08$  dB-sr, respectively. Mean annual rate of pro-

gression of MS,  $V_{TOT}$ , and  $V_{30}$  was  $0.65 \pm 0.46$  dB/year,  $1.55 \pm 0.58$  dB-sr/year, and  $0.92 \pm 0.52$  dB-sr/year, respectively. **Figure 3** shows a representative example of disease progression.

Nine eyes of nine adults (mean age at baseline, 23.1 years; range, 18–32) were included and had a mean follow-up of 21.9 months (range, 12–41 months). Mean baseline MS,  $V_{TOT}$ , and  $V_{30}$  was  $22.11 \pm 4.99$  dB,  $91.33 \pm 20.18$  dB-sr, and  $21.89 \pm 3.69$  dB-sr, respectively. Mean annual rate of progression of MS,  $V_{TOT}$ , and  $V_{30}$  was  $1.01 \pm 0.64$  dB/year,  $2.77 \pm 1.46$  dB-sr/year, and  $0.61 \pm 0.72$  dB-sr/year, respectively.

There was a statistically significant difference between children and adults in mean annual rate of progression of  $V_{TOT}$  ( $P = 0.039$ , independent  $t$ -test) and no statistically significant difference in mean annual rate of progression of MS ( $P = 0.148$ , independent  $t$ -test) and  $V_{30}$  ( $P = 0.259$ , independent  $t$ -test). **Figure 4** illustrates the variability in the annual rate of progression in children and adults.

### Microperimetry

All 43 children and 13 adults with childhood-onset STGD1 underwent microperimetry testing. Three children who were unable to complete the test on either eye and three further children who completed baseline testing on one eye only and had no longitudinal data were excluded from analysis.

### Test-Retest Reliability

A total of 23 children (mean age at baseline, 13.9 years; range, 8–17) underwent microperimetry testing twice at baseline. The ICC values in this subgroup for MS and  $V_{TOT}$  were 0.94 and 0.91, respectively.

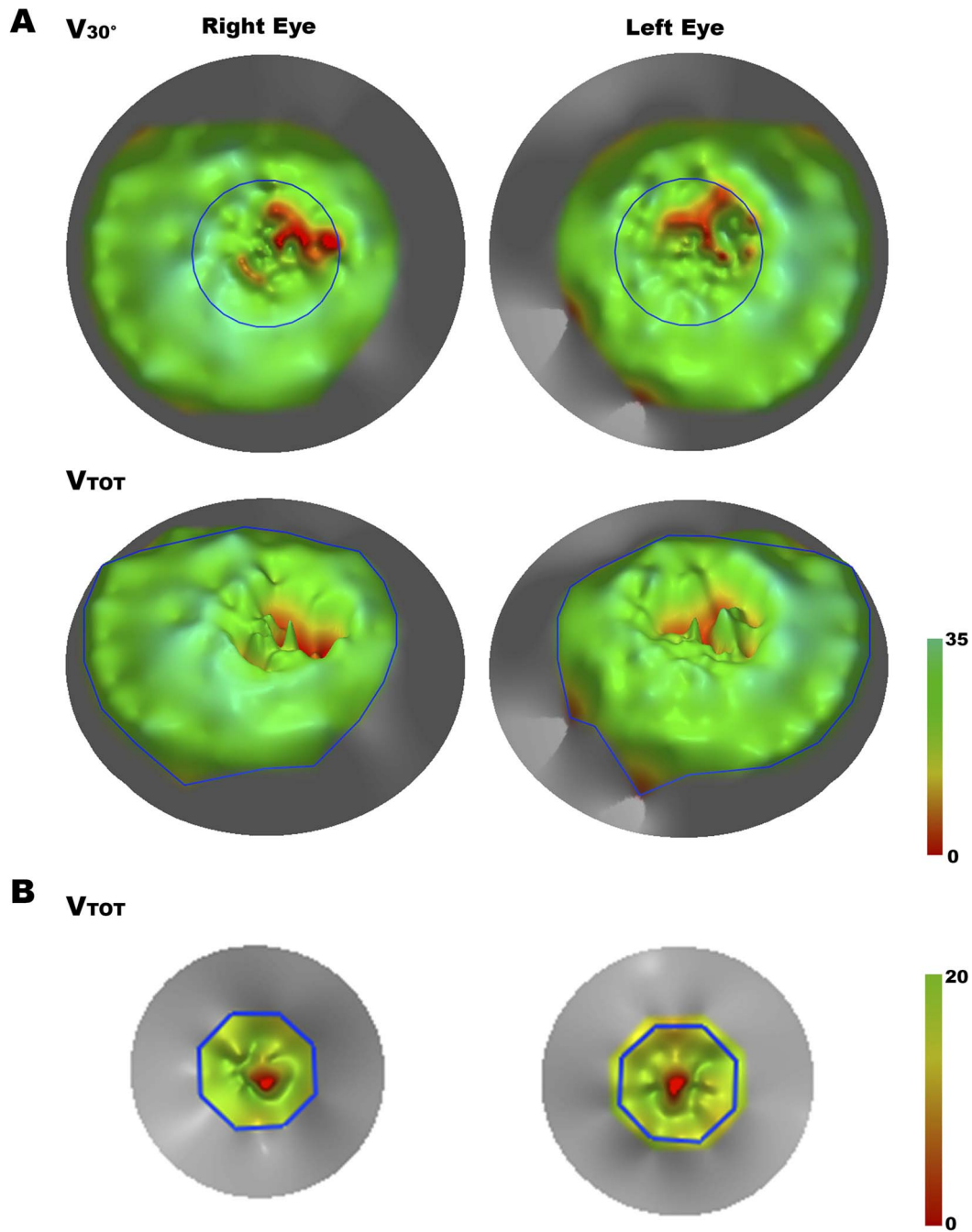


**Figure 2.** Representation of interocular symmetry of perimetry data. (A) VFMA output from full-field static perimetry testing showing disease symmetry in a 17-year-old female with childhood-onset STGD1. *Top Row: Blue circle represents  $V_{30}$ . Middle Row: Blue outline represents  $V_{TOT}$ .* For this subject, the right-eye/left-eye MS values were 25.6/24.7 dB, and the right-eye/left-eye  $V_{TOT}$  and  $V_{30}$  volumes were 101.92/98.65 dB-sr and 19.95/19.45 dB-sr, respectively. Both plots are to the same scale. (B) VFMA output from microperimetry testing showing disease symmetry in a 16-year-old female with childhood-onset STGD1. For this subject, MS and  $V_{TOT}$  results for right eye/left eye were 14.9/15.6 dB and 0.74/0.68 dB-sr, respectively. Both plots are to the same scale.

Eight adults (mean age at baseline, 24.7 years; range, 18–32) underwent microperimetry testing twice at baseline. The ICC values in this subgroup for MS and  $V_{TOT}$  were 0.95 and 0.94 respectively.

#### Interocular Symmetry

Data from 24 children (mean age at baseline, 14.0 years; range, 8–17) and seven adults (mean age at baseline, 22.3 years; range, 18–32) with microperimetry

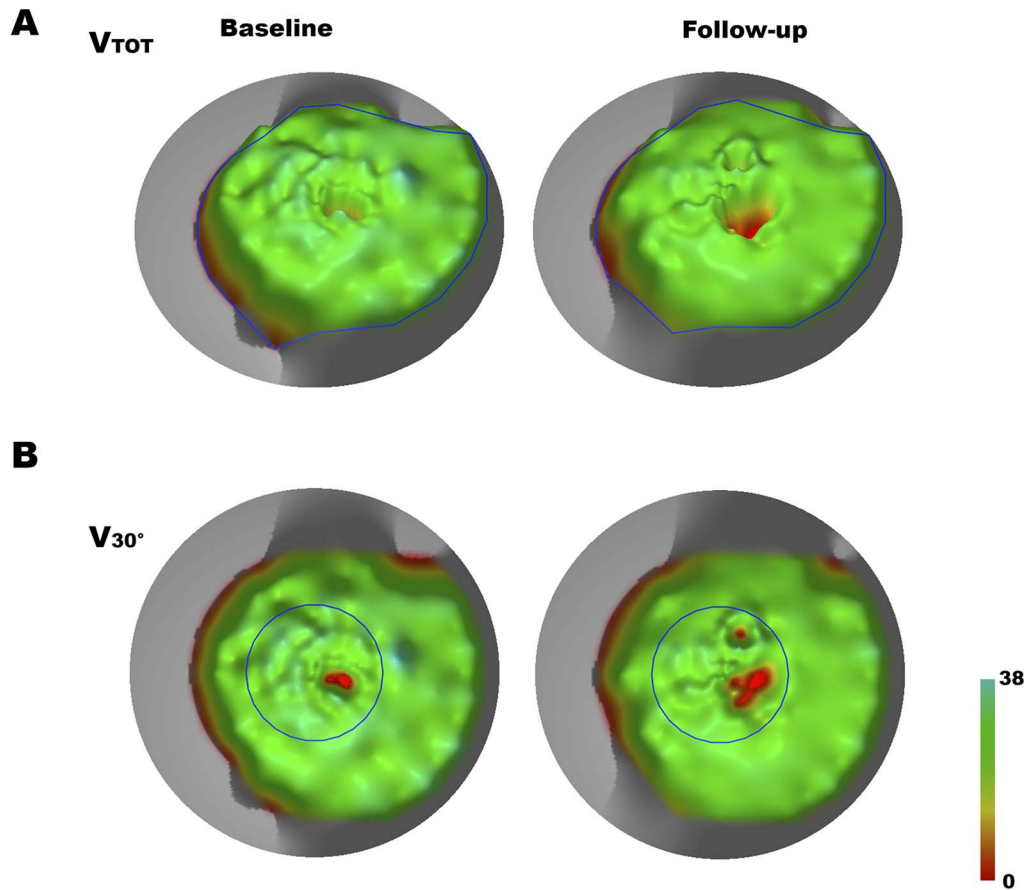


**Figure 3.** Disease progression illustrated by means of full-field static perimetry data from the right eye of a 17-year-old female at baseline and after 29 months of follow-up. (A) Baseline and follow-up measurements of  $V_{TOT}$  were 98.42 dB-sr and 93.03 dB-sr, respectively. (B) Baseline and follow-up measurements of  $V_{30}$  were 24.06 dB-sr and 21.23 dB-sr, respectively. Color scale bar in dB-sr.

etry testing at least once on each eye and a minimum 12-month follow-up were analyzed to assess interocular symmetry.

The subgroup of children showed a strong correlation between eyes in measurements of MS ( $r = 0.94$ ) and  $V_{TOT}$  ( $r = 0.91$ ). There was a strong correlation between eyes in the annual rate of progression of MS ( $r = 0.86$ ) and  $V_{TOT}$  ( $r = 0.80$ ). There was no statistically significant difference between eyes in the baseline measurements of MS ( $P = 0.12$ , paired  $t$ -test) and annual rate of progression of MS ( $P = 0.106$ , paired  $t$ -test). [Figure 2B](#) shows a representative example of interocular symmetry.

The subgroup of adults showed a strong correlation between eyes in measurements of MS ( $r = 0.86$ ) and  $V_{TOT}$  ( $r = 0.85$ ). There was a strong correlation between eyes in the annual rate of progression of MS ( $r = 0.75$ ) and  $V_{TOT}$  ( $r = 0.78$ ). There was no statistically significant difference between eyes in the baseline measurements of MS ( $P = 0.394$ , paired  $t$ -

test) and annual rate of progression of MS ( $P = 0.594$ , paired  $t$ -test).

#### Rate of Progression

Given the lack of statistically significant differences and strong correlations between eyes in the baseline measurements and annual rate of progression, subjects with baseline and follow-up microperimetry testing on at least one eye were assessed subsequently to determine the annual rate of progression. For subjects with serial testing on both eyes, one eye was chosen at random. All subjects had a minimum follow-up of 12 months.

A total of 37 eyes of 37 children (mean age at baseline, 13.2 years; range, 8–17) were included and had a mean follow-up of 24.3 months (range, 12–45 months). Mean baseline MS and  $V_{TOT}$  was  $12.57 \pm 4.27$  dB and  $0.87 \pm 0.39$  dB-sr, respectively. Mean annual rate of progression of MS and  $V_{TOT}$  was  $2.24 \pm 1.12$  dB/year and  $0.21 \pm 0.13$  dB-sr/year, respectively.

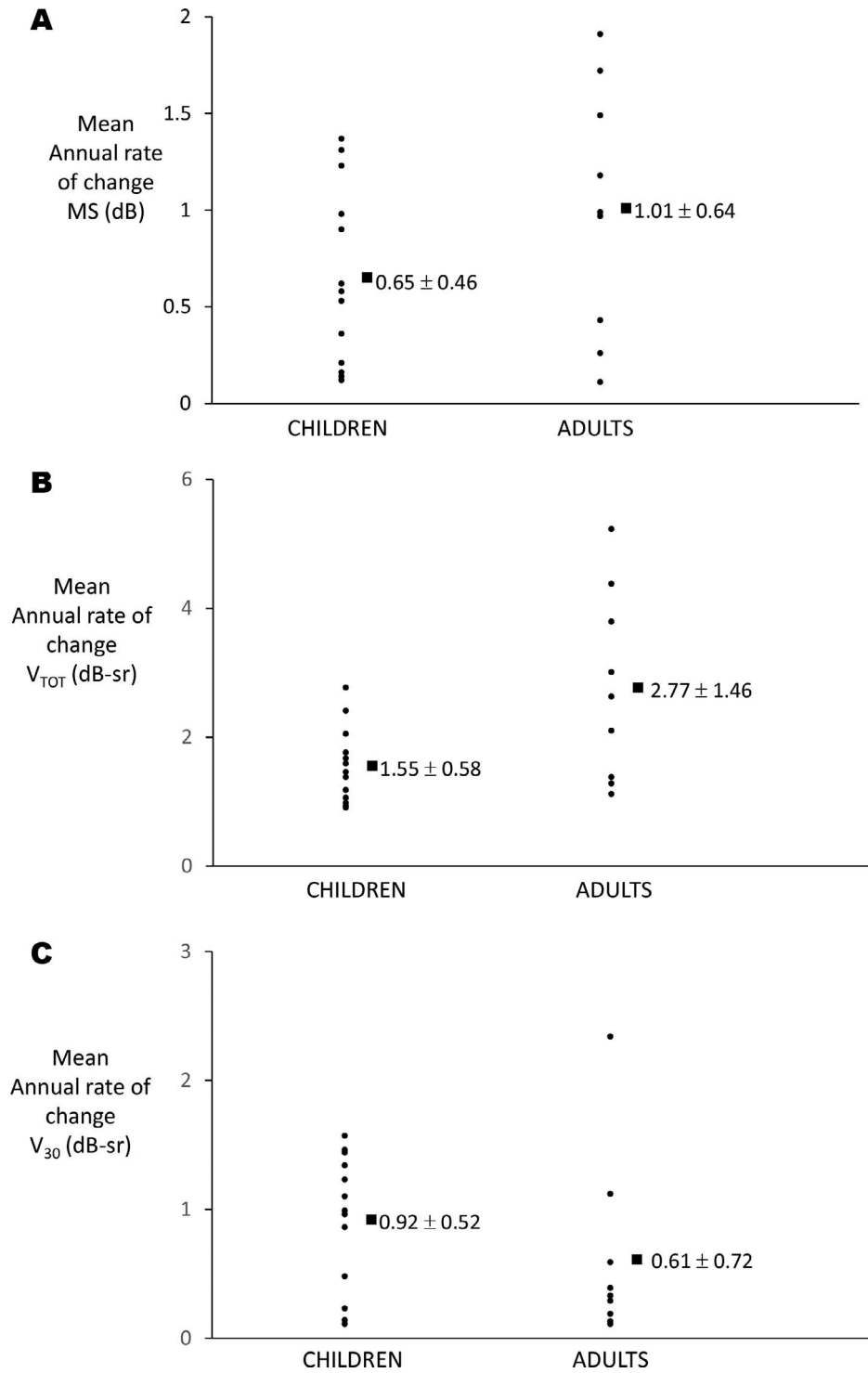


**Figure 4.** Stacked scatterplot showing the variability of the annual rate of change in full-field static perimetry for children and adults. Values represent mean  $\pm$  SD. (A) MS, (B)  $V_{TOT}$ , (C)  $V_{30}$ .

Ten eyes of 10 adults (mean age at baseline, 23.7 years; range, 18–32) were included and had a mean follow-up of 22.7 months (range, 12–41 months). Mean baseline MS and  $V_{TOT}$  was  $8.15 \pm 4.27$  and

$0.52 \pm 0.29$  dB-sr, respectively. Mean annual rate of progression of MS and  $V_{TOT}$  was  $0.82 \pm 0.50$  dB/year and  $0.06 \pm 0.05$  dB-sr/year, respectively.

There was a statistically significant difference

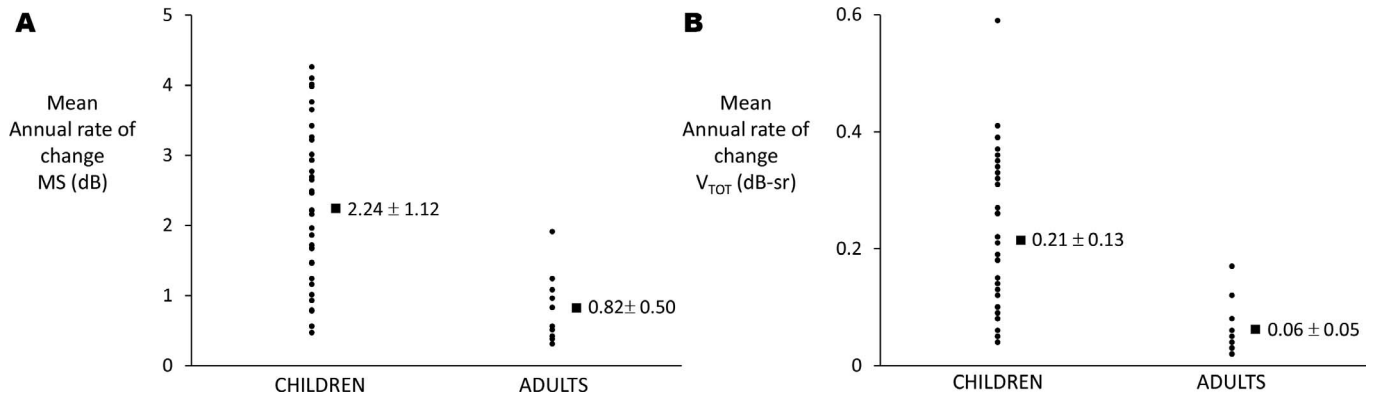


**Figure 5.** Stacked scatterplot showing the variability of the annual rate of change in microperimetry for children and adults. Values represent mean  $\pm$  SD. (A) MS, (B)  $V_{TOT}$ .

between children and adults in mean annual rate of progression of MS ( $P < 0.001$ , independent  $t$ -test) and  $V_{TOT}$  ( $P < 0.001$ , independent  $t$ -test). Figure 5 illustrates the variability in the annual rate of progression in children and adults.

### Correlation Between Perimetry Measurements

The correlation between baseline MS and  $V_{TOT}$  from microperimetry and full-field static perimetry, for adults and children, was tested using the Pearson correlation coefficient. In adults and children, there was a strong positive statistically significant correlation between MS and  $V_{TOT}$  for both tests. For full-field static perimetry, baseline MS and  $V_{TOT}$  showed a strong correlation of  $r = 0.87$  and  $r = 0.91$  for children and adults, respectively. For microperimetry testing, the correlation between baseline MS and  $V_{TOT}$  was  $r = 0.79$  and  $r = 0.88$  for children and adults, respectively.

The baseline  $V_{TOT}$  from microperimetry testing also was tested for correlation with  $V_{30}$  from full-field static perimetry. All eyes for which both metrics were available at baseline were used and tested using the Pearson correlation coefficient. There was a moderate positive statistically significant correlation between the two metrics of  $r = 0.52$  and  $r = 0.65$  for children and adults respectively.

## Discussion

To our knowledge this is the first prospective study of retinal sensitivity in a large cohort of molecularly confirmed childhood-onset STGD1 subjects and highlights the use of microperimetry and full-field static perimetry, as well as volumetric indices of

retinal function, in monitoring disease progression. Furthermore, this study demonstrated that children can reliably undergo serial extensive functional testing.

The Octopus900 and Nidek MP-1 allowed for customizable testing grids and the ability to extract sensitivity data for subsequent topographic analysis using VFMA. Volumetric indices of retinal function derived from topographic analysis provide an alternative to MS when summarizing perimetry data to a single outcome measure. For full-field static perimetry and microperimetry, ICC results for MS and the volumetric indices were good to excellent, indicating strong test-retest reliability. Although MS is a conventional index used to assess perimetry results, it is simply the mathematical average sensitivity value, whereas the decibel-steradian is a physical unit, representing a volume of sensitivity. Moreover, MS may not be an accurate representation of the sensitivity map in certain circumstances. The custom testing grids were radially designed and condensed at the region of interest (central macula). This grid was able to better resolve fine detail in the region of interest, yet had greater coverage compared to a rectilinear grid with the same number of test locations, but with equal intervals between test loci.

Volumetric measures of retinal sensitivity are robust to such custom designs; whereas when grids with unequal spacing are used, the MS value becomes a weighted average that is biased towards the retinal areas with increased test locations. In addition, the MS value can be insensitive to subtle or obvious localized changes, such as foveal sparing. VFMA allows for localized volumetric measurements at specified retinal areas of interest. Three-dimension



modeling of the hill of vision allows for an assessment of the volumetric sensitivity and combined with topographic mapping provides important information from the topographic footprint over which the sensitivity is assessed. Thus, VFMA hill of vision modeling represents a robust and sensitive measure of local changes compared to a single mean value.<sup>28</sup> Despite these limitations, MS still is a reliable measurement, and had a strong correlation with  $V_{TOT}$  for adults and children, and for full-field static perimetry and microperimetry.

In our study two different tests for retinal function were used. The metrics between the two tests are not directly comparable given the different size of the testing areas, and also because of the different number, location and size of testing stimuli. The testing strategy also is different. However, there was a significant correlation between the  $V_{30}$  measured with full-field static perimetry and  $V_{TOT}$  measured with microperimetry. Despite the aforementioned differences, the correlation is arguably not surprising, since both metrics assess similar retinal areas and both are reliable. However, the fact that the correlation was moderate indicated that the measurements were not essentially the same.

Full-field static perimetry data in subjects with STGD1 is limited, possibly due to inherent difficulties in testing subjects, especially children, with low vision. Microperimetry studies also are very limited, as most studies have either investigated microperimetry in heterogeneous subject cohorts, and/or cohorts consisting almost exclusively of adults, and/or are cross-sectional investigations. The only other study assessing perimetry longitudinally in STGD1 showed a progressive reduction of MS, using microperimetry, at an estimated rate of 1.19 dB/year ( $n = 56$ , mean age at baseline of 27.4 years).<sup>30</sup> Notwithstanding the difference in sample size, children in our study showed a significantly higher rate of progression using microperimetry testing compared to the aforementioned study, and also compared to the adult subgroup in our study with childhood-onset STGD1.

ICC results for the children cohort in our study were consistently good to excellent, indicating strong test–retest reliability. We demonstrated that with appropriate support and standardization of instructions, children as young as 13 years are able to complete full-field static perimetry testing and children as young as 8 years are able to complete microperimetry testing. Given the often early onset nature of the disease, additional investigations in

younger children would be valuable to further explore early functional disease progression, and help determine whether children and adults require different testing methods or outcome measures when evaluating retinal function.

Interocular symmetry in terms of baseline measurements and mean annual rate of progression was observed in children and adults with microperimetry and full-field perimetry testing. Establishing that retinal sensitivity progression is symmetrical between eyes is valuable in the design of future treatment strategies where therapeutic intervention often is performed in one eye and compared to the fellow ‘control’ eye. In addition, given that the measurements between eyes are highly correlated, there appears to be equal therapeutic potential for both eyes.

Based on our observation of considerable variability within each subgroup, future studies would benefit from a larger subject cohort, including all subjects repeating baseline testing more than twice. Test–retest variability is likely to vary between subjects depending on factors, such as age, disease duration and disease severity, therefore quantifying individual test–retest variability would ensure a more accurate evaluation of significant changes over time. Increased follow-ups also would provide a more representative rate of progression in retinal sensitivity. Furthermore, the influence of parameters, such as fixation stability and location, also could be explored.

In conclusion, to our knowledge this is the first prospective study of retinal sensitivity in molecularly confirmed childhood-onset STGD1 and highlights the use of full-field static perimetry and microperimetry in monitoring disease progression. Using custom designed grids for full-field static perimetry and microperimetry testing and subsequent topographic analysis, volumetric indices of retinal function provided a reliable measure of change in retinal sensitivity that will be valuable in monitoring subjects in the clinic and moreover, in planned treatment strategies. This study indicated that children with STGD1 can reliably undertake functional testing and may represent good candidates for potential therapeutic interventions. We demonstrated good test–retest reliability and the functional symmetry between eyes in childhood-onset STGD1, and moreover, provided evidence of a significantly greater rate of progression in children compared to adults, both within our study and compared to published data in adults with STGD1.

## Acknowledgments

Supported by grants from the National Institute for Health Research Biomedical Research Centre at Moorfields Eye Hospital NHS Foundation Trust and UCL Institute of Ophthalmology, Macular Society (UK), Moorfields Eye Hospital Special Trustees, Moorfields Eye Charity, Retinitis Pigmentosa Fighting Blindness, The Wellcome Trust (099173/Z/12/Z), and the Foundation Fighting Blindness (USA).

Disclosure: **P. Tanna**, None; **M. Georgiou**, None; **J. Aboshiha**, None; **R.W. Strauss**, None; **N. Kumaran**, None; **A. Kalitzeos**, None; **R.G. Weleber**, named patent holder No.8657449 (P), Scientific Advisory Board for Applied Genetic Technologies Corporation (R), Foundation Fighting Blindness; Scientific Advisory Board for Applied Genetic Technologies Corporation (S); **M. Michaelides**, MeiraGTx (C)

\*PT and MG contributed equally and should be considered equivalent authors.

## REFERENCES

1. Tanna P, Strauss RW, Fujinami K, Michaelides M. Stargardt disease: clinical features, molecular genetics, animal models and therapeutic options. *Br J Ophthalmol*. 2017;101:25–30.
2. Michaelides M, Hunt DM, Moore AT. The genetics of inherited macular dystrophies. *J Med Genet*. 2003;40:641–650.
3. Fujinami K, Lois N, Davidson AE, et al. A longitudinal study of stargardt disease: clinical and electrophysiologic assessment, progression, and genotype correlations. *Am J Ophthalmol*. 2013;155:1075–1088.
4. Fujinami K, Zernant J, Chana RK, et al. Clinical and molecular characteristics of childhood-onset Stargardt disease. *Ophthalmology*. 2015;122:326–334.
5. Strauss RW, Ho A, Munoz B, et al. The natural history of the progression of atrophy secondary to Stargardt Disease (ProgStar) studies: design and baseline characteristics: ProgStar Report No. 1. *Ophthalmology*. 2016;123:817–828.
6. Burke TR, Tsang SH. Allelic and phenotypic heterogeneity in ABCA4 mutations. *Ophthalmic Genet*. 2011;32:165–174.
7. Lambertus S, van Huet RA, Bax NM, et al. Early-onset stargardt disease: phenotypic and genotypic characteristics. *Ophthalmology*. 2015;122:335–344.
8. Allikmets R, Singh N, Sun H, et al. A photoreceptor cell-specific ATP-binding transporter gene (ABCR) is mutated in recessive Stargardt macular dystrophy. *Nat Genet*. 1997;15:236–246.
9. Fujinami K, Zernant J, Chana RK, et al. ABCA4 gene screening by next-generation sequencing in a British cohort. *Invest Ophthalmol Vis Sci*. 2013;54:6662–6674.
10. Zernant J, Schubert C, Im KM, et al. Analysis of the ABCA4 gene by next-generation sequencing. *Invest Ophthalmol Vis Sci*. 2011;52:8479–8487.
11. Haji Abdollahi S, Hirose T. Stargardt-Fundus flavimaculatus: recent advancements and treatment. *Semin Ophthalmol*. 2013;28:372–376.
12. Fishman GA, Stone EM, Grover S, et al. Variation of clinical expression in patients with Stargardt dystrophy and sequence variations in the ABCR gene. *Arch Ophthalmol*. 1999;117:504–510.
13. Rotenstreich Y, Fishman GA, Anderson RJ. Visual acuity loss and clinical observations in a large series of patients with Stargardt disease. *Ophthalmology*. 2003;110:1151–1158.
14. Michaelides M, Chen LL, Brantley MA Jr, et al. ABCA4 mutations and discordant ABCA4 alleles in patients and siblings with bull's-eye maculopathy. *Br J Ophthalmol*. 2007;91:1650–1655.
15. Fujinami K, Sergouniotis PI, Davidson AE, et al. Clinical and molecular analysis of Stargardt disease with preserved foveal structure and function. *Am J Ophthalmol*. 2013;156:487–501.
16. Westeneng-van Haaften SC, Boon CJ, Cremers FP, et al. Clinical and genetic characteristics of late-onset Stargardt's disease. *Ophthalmology*. 2012;119:1199–1210.
17. Burke TR, Tsang SH, Zernant J, Smith RT, Allikmets R. Familial discordance in Stargardt disease. *Mol Vis*. 2012;18:227–233.
18. Singh R, Fujinami K, Chen LL, Michaelides M, Moore AT. Longitudinal follow-up of siblings with a discordant Stargardt disease phenotype. *Acta Ophthalmol*. 2014;92:e331–e332.
19. Fujinami K, Lois N, Mukherjee R, et al. A longitudinal study of Stargardt disease: quantitative assessment of fundus autofluorescence, progression, and genotype correlations. *Invest Ophthalmol Vis Sci*. 2013;54:8181–8190.
20. Smith J, Ward D, Michaelides M, Moore AT, Simpson S. New and emerging technologies for the treatment of inherited retinal diseases: a horizon scanning review. *Eye (Lond)*. 2015;29:1131–1140.

21. Schwartz SD, Regillo CD, Lam BL, et al. Human embryonic stem cell-derived retinal pigment epithelium in patients with age-related macular degeneration and Stargardt's macular dystrophy: follow-up of two open-label phase 1/2 studies. *Lancet*. 2015;385:509–516.
22. Dalkara D, Goureau O, Marazova K, Sahel JA. Let there be light: gene and cell therapy for blindness. *Hum Gene Ther*. 2016;27:134–147.
23. Saad L, Washington I. Can vitamin A be improved to prevent blindness due to age-related macular degeneration, Stargardt disease and other retinal dystrophies? *Adv Exp Med Biol*. 2016;854:355–361.
24. Chen FK, Patel PJ, Xing W, et al. Test-retest variability of microperimetry using the Nidek MP1 in patients with macular disease. *Invest Ophthalmol Vis Sci*. 2009;50:3464–3472.
25. Cideciyan AV, Swider M, Aleman TS, et al. Macular function in macular degenerations: repeatability of microperimetry as a potential outcome measure for ABCA4-associated retinopathy trials. *Invest Ophthalmol Vis Sci*. 2012;53:841–852.
26. Chen FK, Patel PJ, Webster AR, et al. Nidek MP1 is able to detect subtle decline in function in inherited and age-related atrophic macular disease with stable visual acuity. *Retina*. 2011;31:371–379.
27. Cideciyan AV, Swider M, Aleman TS, et al. ABCA4-associated retinal degenerations spare structure and function of the human parapapillary retina. *Invest Ophthalmol Vis Sci*. 2005;46:4739–4746.
28. Weleber RG, Smith TB, Peters D, et al. VFMA: Topographic analysis of sensitivity data from full-field static perimetry. *Transl Vis Sci Technol*. 2015;4:14.
29. Schiefer U, Pascual JP, Edmunds B, et al. Comparison of the new perimetric GATE strategy with conventional full-threshold and SITA standard strategies. *Invest Ophthalmol Vis Sci*. 2009;50:488–494.
30. Testa F, Melillo P, Di Iorio V, et al. Macular function and morphologic features in juvenile stargardt disease: longitudinal study. *Ophthalmology*. 2014;121:2399–2405.